

Isoscalar giant resonance strength in ^{28}Si

D. H. Youngblood, Y.-W. Lui, and H. L. Clark

Cyclotron Institute, Texas A&M University, College Station, Texas 77843, USA

(Received 7 May 2007; published 28 August 2007)

Data taken previously covering the giant resonance region from $9 \text{ MeV} < E_x < 42 \text{ MeV}$ in ^{28}Si with inelastic scattering of 240 MeV α particles at small angles including 0° have been reanalyzed. Treating all of the observed cross section as multipole processes, giant resonance peaks containing $74 \pm 7\%$ of the isoscalar $E0$ energy weighted sum rule (EWSR), $102 \pm 11\%$ of the $E2$ EWSR, and $84 \pm 8\%$ of the $E3$ EWSR were identified.

DOI: [10.1103/PhysRevC.76.027304](https://doi.org/10.1103/PhysRevC.76.027304)

PACS number(s): 24.30.Cz, 25.55.Ci, 27.30.+t

The properties of the isoscalar giant resonances in nuclei are important because of what they tell us of the bulk nuclear properties. The isoscalar giant monopole resonance (GMR) is of particular importance because its energy can be directly related to the nuclear compressibility and from this the compressibility of nuclear matter (K_{NM}) can be obtained. We have reported previous studies [1,2] of the giant resonance region in ^{28}Si using inelastic scattering of 240 MeV α particles at small angles including 0° . These studies have focused on obtaining the parameters of the GMR, and strength corresponding to $81 \pm 10\%$ of the isoscalar $E0$ EWSR has been identified. Strength corresponding only to $15 \pm 4\%$ of the isoscalar $E1$ EWSR and $68 \pm 9\%$ of the $E2$ EWSR were identified in ^{28}Si . Higher multipoles were not distinguished. However in somewhat heavier nuclei such as ^{40}Ca [3], $E0$ and $E2$ strengths have consistent with 100% of the EWSR were identified, while in medium and heavy nuclei [4] all or most of the expected isoscalar $E0$, $E1$, $E2$, and $3\hbar\omega E3$ strengths have been identified. In all of these analyses a continuum chosen (arbitrarily) to represent processes other than multipole excitation was subtracted from the spectra before the analysis was carried out. There was some effort to determine the extent of $E0$ strength in this “continuum” and this “continuum” $E0$ strength was included in the $E0$ strengths reported. In our more recent analyses this continuum was varied systematically, and the effects on the multipole distributions assessed and included in determinations of the distributions and their errors. However, the Si analyses reported in Refs. [1,2] preceded the development of codes which made a systematic study of the effects of continuum changes practical, so at most a couple of continua were tried. We report here an analysis of the ^{28}Si data reported in Ref. [1] up to an excitation energy of 42 MeV where the assumption was made that ALL of the cross sections are due to multipole processes. Alpha particles from the decay of the mass 5 ejectile created in the $(\alpha, ^5\text{He})$ and $(\alpha, ^5\text{Li})$ reactions will be a competing process above $E_x = 42 \text{ MeV}$ (^5Li) and 50 MeV (^5He), so this “zero continuum” analysis would not be appropriate above $E_x = 42 \text{ MeV}$.

The experimental technique was described in Ref. [1] and is summarized briefly below. A beam of 240 MeV α particles from the Texas A&M K500 superconducting cyclotron bombarded a self-supporting natural silicon wafer 7.92 mg/cm^2 thick located in the target chamber of the multipole-dipole-multipole spectrometer. The horizontal acceptance of the

spectrometer was 4° and ray tracing was used to reconstruct the scattering angle. The out-of-plane scattering angle was not measured. Data were taken at spectrometer angles of 0° , 3.5° , and 5.5° , covering from 0° to 7.4° in the center of mass. Sample spectra are shown in Fig. 1 and the continua used for the analyses in Ref. [1] are shown. In the analysis reported below, we assumed that all α particles detected that corresponded to excitation energies below $E_x = 42 \text{ MeV}$ came from multipole processes having $L \leq 4$.

The multipole components were obtained [1] by dividing the data into multiple regions (bins) by excitation energy and then comparing the angular distributions obtained for each of these bins to distorted wave Born approximation (DWBA) calculations to obtain the multipole components. The uncertainty from the multipole fits was determined for each multipole by incrementing (or decrementing) that strength, then adjusting the strengths of the other multipoles to minimize total χ^2 . This continued until the new χ^2 was 1 unit larger than the total χ^2 obtained for the best fit.

The DWBA calculations were described in Ref. [1] and the same density dependent Woods-Saxon folding potentials were used for the calculations in this work. A sample of the angular distributions obtained are shown in Fig. 2. Fits to the angular distributions were carried out with a sum of isoscalar 0^+ , 1^- , 2^+ , 3^- , and 4^+ strengths. The limited angular range of the data prevents distinguishing $L = 4$ and higher contributions. The isovector giant dipole resonance (IVGDR) contributions are small, but were calculated from the known distribution [5] and held fixed in the fits. Sample fits obtained, along with the individual components of the fits, are shown superimposed on the data in Fig. 2.

The strength distributions obtained for isoscalar $L = 0, 1, 2, 3$, and 4 are shown in Fig. 3. The $E0$ multipole distribution is superimposed on the distribution from Ref. [1]. They are in reasonable agreement over the entire energy region. The EWSR strength obtained, $74 \pm 7\%$ of the $E0$ EWSR, the centroid energy ($m1/m0$) $20.89 \pm 0.38 \text{ MeV}$ and rms width $5.9 \pm 0.6 \text{ MeV}$ all agree within the errors with those from Ref. [1] ($81 \pm 10\%$, $21.25 \pm 0.38 \text{ MeV}$, and $6.4 \pm 0.6 \text{ MeV}$, respectively). This work and Ref. [1] used the same data, DWBA calculations, and fitting routines so that the small differences can be attributed entirely to the choice of continuum. This suggests that the extracted monopole strength is only weakly dependent on the assumptions made about the

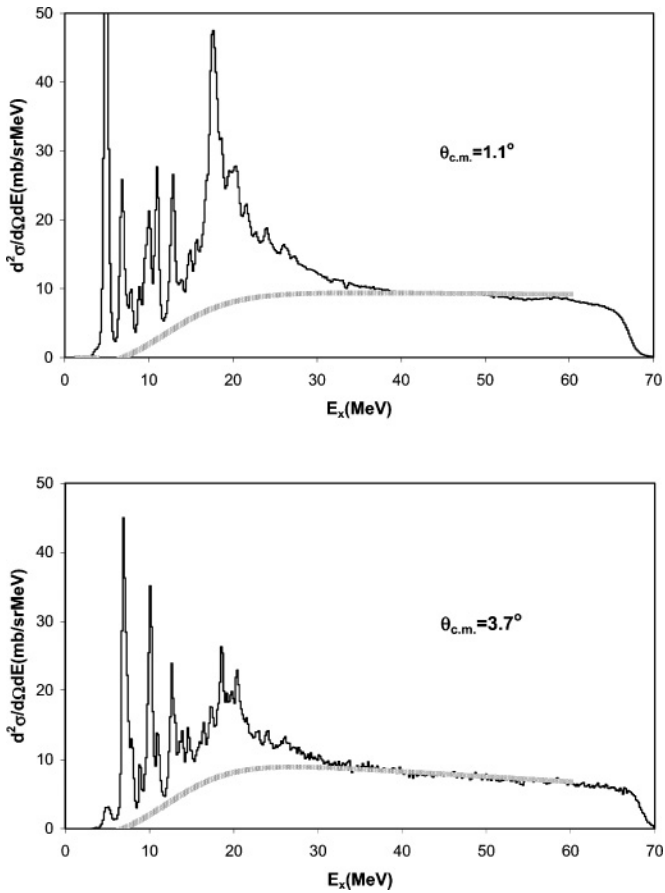


FIG. 1. Inelastic α spectra (reported in Ref. [1]) obtained with the spectrometer at average c.m. angles of 1.1° and 3.7° . The thick gray lines show the continuum used for the analysis in Ref. [1].

continuum, which we have seen in analyses of data for other nuclei. This is not true for other multiplicities.

In the region $E_x = 9\text{--}35$ MeV, $E2$ strength corresponding to $102 \pm 11\%$ of the $E2$ EWSR was identified in a broad peak with a centroid of 18.77 ± 0.35 MeV and rms width of 5.45 ± 0.20 MeV. This contrasts sharply with the results of Ref. [1] (shown for comparison in Fig. 3) where after a continuum was subtracted, $E2$ strength was identified corresponding to $68 \pm 9\%$ of the $E2$ EWSR. The centroid and rms width of the $E2$ strength reported in Ref. [1] were 18.54 ± 0.25 MeV and 4.7 ± 0.6 MeV suggesting that the additional strength identified in this analysis lies predominantly in the higher energy region as might be expected since the continuum assumed in Ref. [1] was lower at lower excitation. Earlier works [2,6–8] had generally identified $\leq 32\%$ of the $E2$ EWSR centered at $E_x \sim 19.4$ MeV. The known 2^+ strength in states below $E_x \sim 9.5$ MeV corresponds to $\sim 11.4\%$ of the $E2$ EWSR [9], so that all of the expected isoscalar $E2$ strength in ^{28}Si is accounted for below 35 MeV. Above $E_x = 35\text{--}38$ MeV the $E2$ strength appears to increase up to the highest energy analyzed apparently containing another 27% of the $E2$ EWSR. We believe this to be due to unidentified continuum processes that have distributions similar to an $L = 2$ multipole.

$E3$ strength in nuclei is divided [10] between $1\hbar\omega$ strength at low excitation ($\sim 25\%$ of the $E3$ EWSR) and $3\hbar\omega$ strength

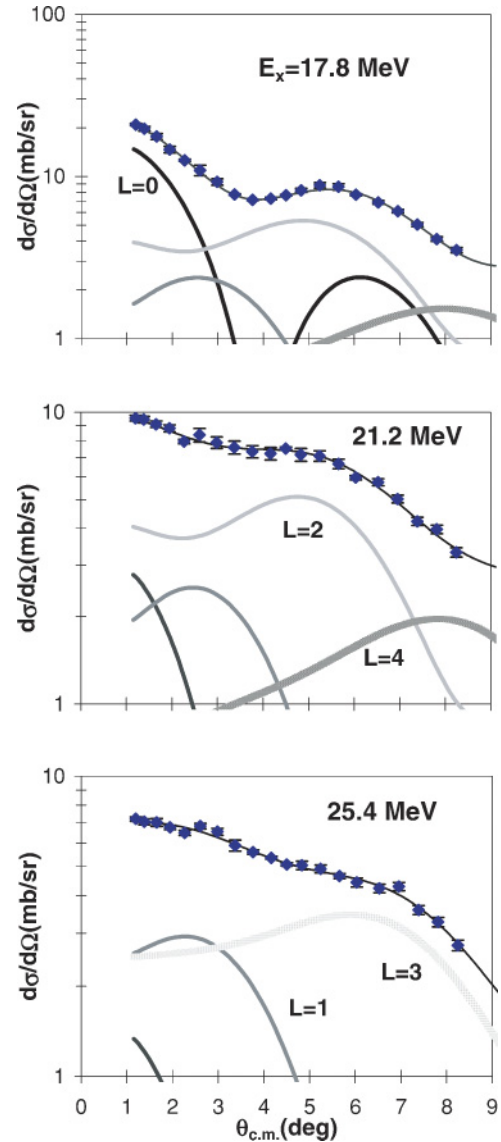


FIG. 2. (Color online) Angular distributions obtained for inelastic α scattering for three excitation ranges in ^{28}Si . The energy bins are approximately 450 keV wide. The medium black lines show the fits. Contributions of each multipole are shown. When not shown, errors are smaller than the data points.

at higher excitation ($\sim 75\%$ of the $E3$ EWSR). As can be seen in Fig. 3, our analysis shows a small amount of $E3$ strength between 10 and 18 MeV (3% of the $E3$ EWSR) and a much larger amount ($81 \pm 8\%$ of the $E3$ EWSR) between 23 and 39 MeV centered at 32 MeV with an rms width of 5.3 ± 0.4 MeV. Only small amounts of $E3$ strength have been seen in other nuclei with $A < 56$. In the mass 56–64 region, $E3$ strength was not separated from higher multipoles, but the total $L \geq 3$ strength seen was between 87–100% of the $E3$ EWSR [11]. In heavier nuclei ($A = 90\text{--}208$) where $E3$ strength was separated from $L \geq 4$ strength, approximately 75% of the $E3$ EWSR was identified at higher excitation [4] and $E_{\text{HEOR}} * A^{1/3}$ lies between 92 and 116 MeV. The observed HEOR strength in ^{28}Si corresponds to $E_{\text{HEOR}} * A^{1/3} = 95$ MeV. Thus this higher

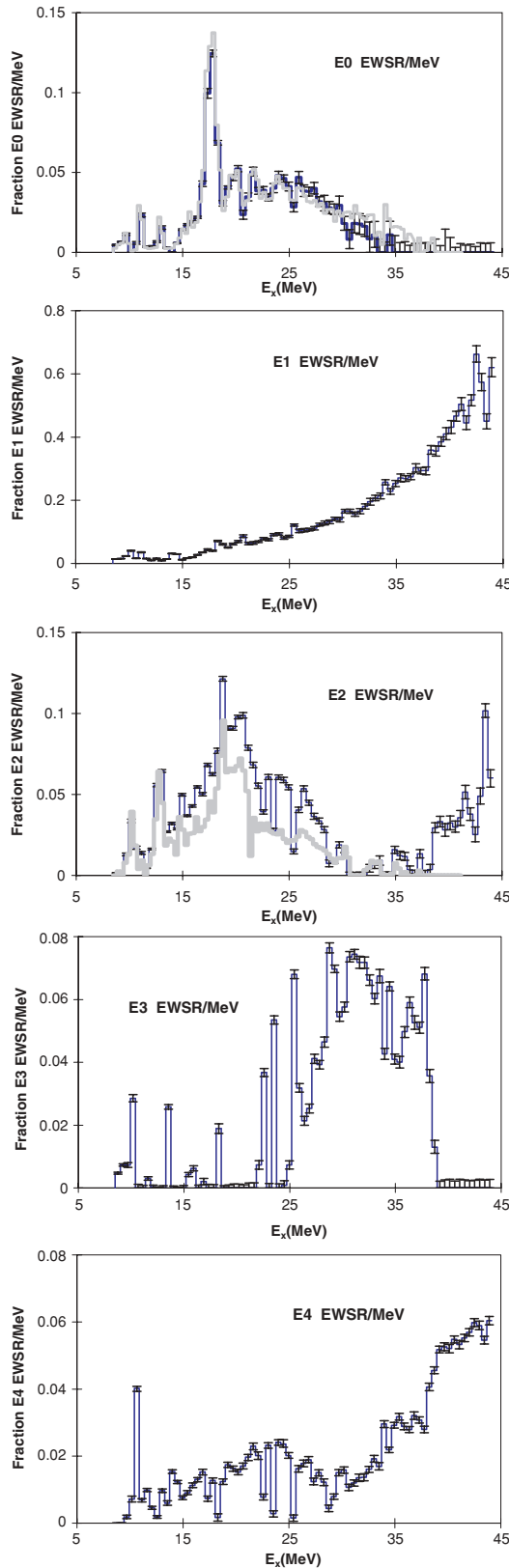


FIG. 3. (Color online) The $E0$, $E1$, $E2$, $E3$, and “ $E4$ ” strength distributions obtained are shown by the black histograms. Error bars represent the uncertainty due to the fitting of the angular distributions as described in the text. The grey histograms show the $E0$ and $E2$ distributions reported in Ref. [1].

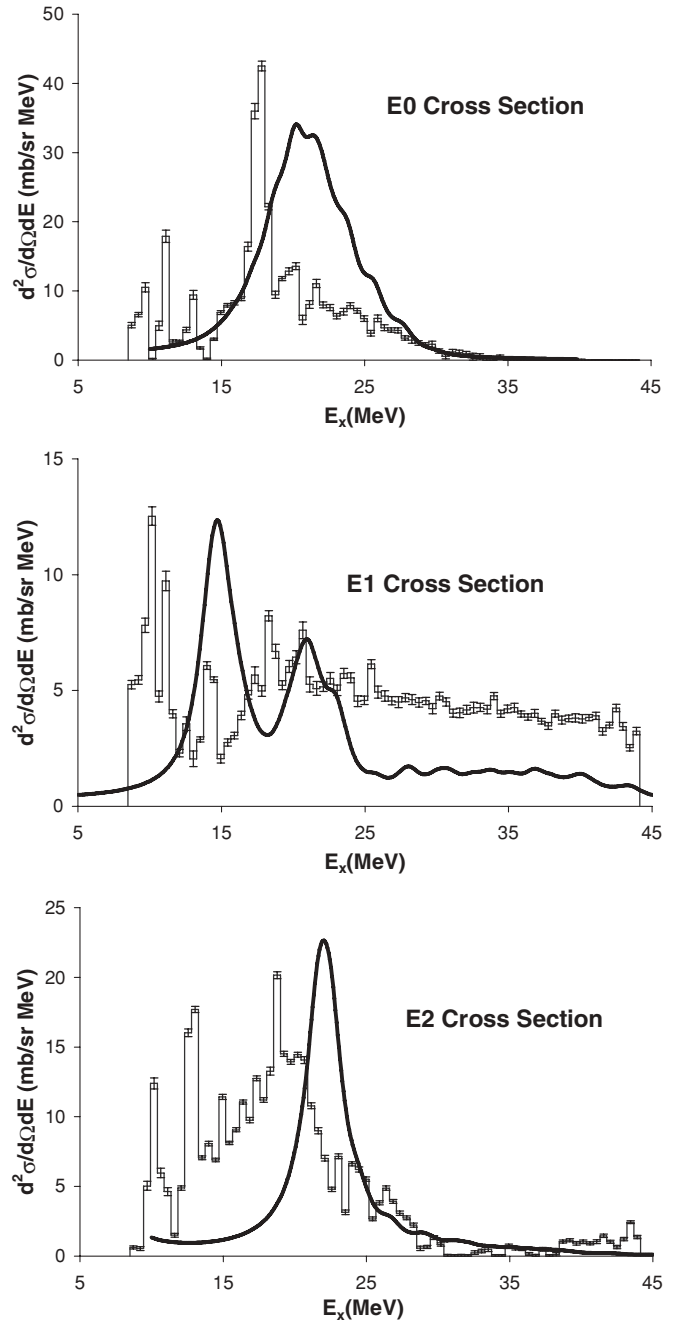


FIG. 4. (Color online) Cross sections (at the peak of the angular distributions) for $E0$, $E1$, and $E2$ excitation (obtained from the strength distributions shown in Fig. 3) are shown by the histograms. The solid lines are calculations from Ref. [12].

$E3$ strength is consistent with what is expected for the $3\hbar\omega$ component of the $E3$ strength in ^{28}Si .

The “ $E4$ ” ($L \geq 4$) strength has a broad peak between 9 and 30 MeV followed by a dramatic increase above $E_x = 30$ MeV. The total strength observed corresponds to $\sim 80\%$ of the $E4$ EWSR, but the relatively fast increase above 30 MeV is likely due to continuum processes having relatively flat angular distributions.

The “isoscalar $E1$ strength” obtained rises sort of smoothly from 9 MeV to 40 MeV and corresponds to 140% of the

isoscalar $E1$ EWSR. In the analysis reported in Ref. [1] as well as analyses of the data for other nuclei [4], the isoscalar $E1$ strength extracted from a multipole analysis of the continuum rises almost monotonically up to the highest excitation energy studied and corresponds to significantly more than the sum rule strength. There are likely continuum processes which are responsible for much of this (apparent) $E1$ strength as discussed below.

In Fig. 4 the $E0$, $E1$, and $E2$ strength functions from Fig. 3 have been converted into cross section at the peak of the angular distribution. Also plotted are Hartree-Fock random phase approximation calculations [12] for strength distributions converted to cross sections (at the peak of the angular distribution for each multipole) using double folding calculations where the transition densities for each multipole were obtained from the HF-RPA calculations. These calculations did not include specific nuclear structure effects and show no structure whereas in this light nucleus considerable

structure is present in the data as expected. The centroids of the calculated $E0$ and $E2$ strengths are somewhat above those for the data, which might be expected from the lack of inclusion of nuclear structure effects. It would appear that the same might be true for the $E1$ strength, as the peaks in the calculated spectrum would crudely agree with the data if the calculated cross sections were shifted down about 4 MeV. Above $E_x \sim 25$ MeV the $E1$ double differential cross section is about 50% of the observed cross section for all processes and is ~ 2.5 times the predicted cross section, suggesting that some (significant?) part of the data is not due to $E1$ excitation but other (unidentified) processes that somewhat mimic an $E1$ angular distribution.

This work was supported in part by the U.S. Department of Energy under grant No. DE-FG03-93ER40773 and by The Robert A. Welch Foundation under grant No. A-0558.

-
- [1] D. H. Youngblood, Y.-W. Lui, and H. L. Clark, Phys. Rev. C **65**, 034302 (2002).
 - [2] D. H. Youngblood, H. L. Clark, and Y.-W. Lui, Phys. Rev. C **57**, 1134 (1998).
 - [3] D. H. Youngblood, Y.-W. Lui, and H. L. Clark, Phys. Rev. C **63**, 067301 (2001).
 - [4] D. H. Youngblood, Y.-W. Lui, H. L. Clark, B. John, Y. Tokimoto, and X. Chen, Phys. Rev. C **69**, 034315 (2004); **69**, 054312 (2004).
 - [5] S. S. Dietrich and B. L. Berman, At. Data Nucl. Data Tables **38**, 199 (1988).
 - [6] K. T. Knopfle *et al.*, Phys. Lett. **B64**, 263 (1976).
 - [7] K. Van der Borg, M. N. Harakeh, and A. Van der Woude, Nucl. Phys. **A365**, 243 (1981).
 - [8] Y. W. Lui, J. D. Bronson, D. H. Youngblood, Y. Toba, and U. Garg, Phys. Rev. C **31**, 1643 (1985).
 - [9] P. M. Endt, Nucl. Phys. **A633**, 1 (1998); interim evaluation, B. Singh (2001); data extracted from the ENSDF database, revision of July 24, 2003, NNDC.
 - [10] J. M. Moss, D. H. Youngblood, C. M. Rozsa, D. R. Brown, and J. D. Bronson, Phys. Rev. Lett. **37**, 816 (1976).
 - [11] Y.-W. Lui, D. H. Youngblood, H. L. Clark, Y. Tokimoto, and B. John, Phys. Rev. C **73**, 014314 (2006).
 - [12] S. Shlomo, B. Debresch, A. I. Sanzhur, and A. Moalem (private communication).